Multi-user interference cancellation schemes for carrier frequency offset compensation in uplink OFDMA

Nguyen, Huan Cong; De Carvalho, Elisabeth; Prasad, Ramjee

Published in:
IEEE Transactions on Wireless Communications

DOI (link to publication from Publisher):
10.1109/TWC.2014.021414.070718

Publication date:
2014

Document Version
Early version, also known as pre-print

Multi-user interference cancellation schemes for carrier frequency offset compensation in uplink OFDMA

Journal:	*IEEE Transactions on Wireless Communications*
Manuscript ID:	Paper-TW-Jul-07-0718.R1
Manuscript Type:	Original Transactions Paper
Date Submitted by the Author:	13-Nov-2007
Complete List of Authors:	Nguyen, Huan; Aalborg University, Electronic Systems De Carvalho, Elisabeth; Aalborg Univeristy, Electronic Systems Prasad, Ramjee; Aalborg University, Electronic Systems
Keyword:	Multiuser detection < Transmission Technology, Synchronization < Transmission Technology, Transceiver Design < Transmission Technology, Multiple access techniques < Wireless Access

Multi-user interference cancellation schemes for carrier frequency offset compensation in uplink OFDMA

Huan Cong Nguyen, Elisabeth de Carvalho and Ramjee Prasad

ABSTRACT

Each user in the uplink of an Orthogonal Frequency Division Multiple Access (OFDMA) system may experience a different carrier frequency offset (CFO). These uncorrected CFOs destroy the orthogonality among subcarriers, causing inter-carrier interference and multi-user interference, which degrade the system performance severely. In this paper, novel time-domain multi-user interference cancellation schemes for OFDMA uplink are proposed. They employ an architecture with multiple OFDMA-demodulators to compensate for the impacts of multi-user CFOs at the BS's side. Analytical and numerical evaluations show that the proposed schemes achieve a significant performance gain compared to the conventional receiver and a reference frequency-domain multi-user interference cancellation scheme. In a particular scenario, a maximum CFO of up to 40% of the subcarrier spacing can be tolerated, and the CFO-free performance is maintained in the OFDMA uplink. The proposed schemes outperform the multi-user interference cancellation techniques for Orthogonal Frequency Division Multiple Access (OFDMA) available in literature with comparable or lower complexity.

Index Terms

Synchronization, OFDMA, uplink, timing offset, frequency offset, multiuser interference cancellation.

I. INTRODUCTION

In recent years, Orthogonal Frequency Division Multiple Access (OFDMA) has emerged as the primary transmission and multiple access scheme for broadband wireless networks. It has been adopted as the Physical Layer (PHY) layer for different broadband wireless networks standards, including the IEEE 802.16 (WiMax), ETSI HiperMAN and SK Telecom's WiBro. OFDMA is also now a part of the Universal Mobile Telecommunications System (UMTS), the European standard for the 3^{rd} Generation

(3G) cellular mobile communications. Being a multi-user version of the famous Orthogonal Frequency Division Multiplexing (OFDM) technique, OFDMA operates by separating data into multiple lower-rate streams and transmitting them in parallel over orthogonal carrier frequencies, or subcarriers. Due to the orthogonality, those subcarriers are allowed to overlap in the frequency-domain, therefore high spectral efficiency can be achieved. The low-rate parallel subcarriers transmission turns multipath fading channels into flat fading ones, thus simplifying the equalization task at the receiver. In OFDMA, available subcarriers are grouped into sub-channels, which are assigned to different users operating simultaneously. This allows a finer granularity for multiple access, compared to Orthogonal Frequency Division Multiplexing - Time Division Multiple Access (OFDM-TDMA) multiple access scheme, in which all subcarriers are given to one user only at any given time.

OFDMA inherits from OFDM its sensitivity to Carrier Frequency Offset (CFO) and phase noise [1]. The carrier frequency mis-alignment destroys the orthogonality of the subcarriers, which causes Inter-Carrier Interference (ICI) and consequently produces Multi-User Interference (MUI) among users [2]. While the CFO can be estimated and corrected relatively easily in the downlink, preserving orthogonality in the uplink is much more demanding. In the uplink, the received signal is the sum of multiple signals coming from different users, each of which experiences a different CFO due mainly to oscillator instability and/or Doppler shift [3]. These relative CFOs among users must be corrected, otherwise the system performance degrades severely. Downlink CFO correction methods, which are designed for single-user scenario, are unable to correct multiple CFOs in the uplink, as correction to one user's CFO would misalign the other users [4].

Various studies have been carried out to tackle the multiple CFO problems in the OFDMA uplink scenario, which can be divided into two categories: Interference Avoidance (IA) and Interference Cancellation (IC) methods. Examples of IA schemes includes windowing, self-ICI cancellation and feedback-and-adjust approaches. The windowing approach in [5], [6] shapes the output of the Inverse Discrete Fourier Transform (IDFT) by a window to suppress the side-lobes of the subcarriers, thus reduces the sensitivity to frequency errors. This approach normally causes Carrier to Noise Ratio (CNR) loss, and ICI in the case of no CFOs [7]. The self-ICI cancellation approach is performed in frequency-domain, where a set of codewords with low ICI is used to reduce the side-lobes of the output spectrum. Since the code rate is less than one, the spectrum efficiency is reduced [8]. The feedback-and-adjust schemes are described in [3], [4], which suggest that the Base Station (BS) performs only Timing Offset (TO) and CFO estimation, whereas adjustment of the synchronization parameters is made at the Mobile Station (MS)'s side based on instruction transmitted on the BS's control channel. The feedback-and-adjust approach requires an established connection between BS and MS, which is not applicable for some scenarios, and additional signalling overhead, which reduces

the system throughput. Also note that, in this approach, there is always a delay between the estimation and adjustment processes, during which the CFO estimation can be outdated (e.g. because of Doppler frequencies) [9].

On the other hand, the IC schemes aim at removing the unwanted ICI and recovering the ideal waveform: In [10], [11], a multiple CFOs estimation and compensation algorithm is introduced based on subspace method. This scheme works only with interleaved subcarrier allocation. A linear multiuser detection scheme is proposed in [2], hereby referred to as Cao-Tureli-Yao-Honan (CTYH), which attempts to restore the orthogonality among users by applying a linear transformation to the Fast Fourier Transform (FFT) output. The interference due to CFOs is suppressed at the price of additional complexity [12]. In [9], a MUI cancellation scheme in frequency-domain is proposed, hence it is referred to as Frequency-Domain Multi-User Interference Cancellation (FD-MUIC) in this paper. In this scheme, circular convolutions are employed after the FFT processing to correct the CFOs, and to calculate the MUI terms, which are then subtracted from the subcarrier of interest. This scheme suffers from the loss of subcarrier's power when the CFOs are large, and it is unable to completely remove the self-ICI, which occurs among subcarriers of the same user [9].

In this paper, we propose simple but effective IC schemes to mitigate the effects of different CFOs coming from multiple users in the uplink of OFDMA systems. The proposed schemes consist of two stages: Prior to uplink transmission, MS performs a coarse synchronization to BS, using well-known single-user CFO estimation techniques, such as [13], [14], so that the CFO is within a tolerable range. In the second stage, novel signal processing techniques are employed at the BS's side to estimate and correct the residual CFOs, and to compensate for the ICI. The ICI compensation is performed in time-domain, thus our proposals are hereafter referred to as Time-Domain Multi-User Interference Cancellation (TD-MUIC) schemes. No further adjustment at MS's side is needed, thus, no additional signalling overhead is required. The maximum tolerable CFO can be as large as 25% of the subcarrier spacing, which is a significant improvement compared to the stringent requirement in Institute of Electrical and Electronics Engineers (IEEE) 802.16a, which is 2% of the subcarrier spacing [15]. A loose CFO requirement means low-cost and simple terminals are allowed in the system. The scheme works with both block and interleaved subcarrier allocations, and does not require special processing block, except the basic and readily-available FFT. Analytical and numerical results show that the proposed schemes offer much better performance compared to the FD-MUIC scheme.

This paper is organized as follows. The system model and conventional receiver structures for the OFDMA uplink are presented in Section II. Section III provides the proposed schemes, along with numerical evaluation assuming perfect CFO knowledge. Simulation results with a practical CFO estimation technique are reported in Section IV, and finally conclusions are drawn in Section V.

II. Uplink OFDMA receiver structures

Let's consider an OFDMA system using a FFT of size N. In this system, the u^{th} user is given a set of subcarriers, denoted as Δ_u, which is independent from the other users, i.e. $\Delta_u \bigcap \Delta_{u'} = \emptyset$ for $u \neq u'$. The transmitted information of the u^{th} user, after Inverse Fast Fourier Transform (IFFT) operation and Cyclic Prefix (CP) insertion, is given by:

$$x_u(t) = \frac{1}{N} \sum_{k \in \Delta_u} X_u[k] e^{j2\pi \frac{k}{T_o}(t-T_g)} \Xi_{T_s}(t) \tag{1}$$

where T_o is the OFDMA symbol duration without guard interval, T_g is the guard interval, and $\Xi_{T_s}(t)$ is the unity amplitude gate pulse of length $T_s = T_o + T_g$. $X_u[k]$ denotes the information symbol for the k^{th} subcarrier of the u^{th} user. We assume that the transmitted symbols on each subcarrier have zero mean and are uncorrelated, i.e. $E\{X_u[k]\} = 0$ and:

$$E\{X_u[k] X_{u'}[k']^*\} = \begin{cases} \sigma^2_{X_u} & \text{for } u = u', k = k' \\ 0 & \text{otherwise} \end{cases} \tag{2}$$

Assume that the u^{th} user experiences an independent TO, δt_u, and frequency-selective fading channel, which are constant during the observation period, the received signal from the u^{th} user is:

$$y_u(t) = \sum_{l=0}^{L-1} h_{u,l} x_u(t - \delta t_u - \tau_{u,l}) \tag{3}$$

where $h_{u,l}$ and $\tau_{u,l}$ are the complex gain and time delay of the l^{th} multipath component experienced by the u^{th} user, respectively. In the OFDMA uplink, the received signal is the sum of the signal from multiple users, which can be expressed as:

$$r(t) = \sum_{u=0}^{U-1} y_u(t) e^{j2\pi \delta f_u t} + v(t) \tag{4}$$

where δf_u is the CFO of the u^{th} user and $v(t)$ is the complex baseband Additive White Gaussian Noise (AWGN) at the input of the OFDMA receiver.

At the receiver, the received signal is sampled at rate $1/\Delta t$ and the CP is removed to form the received vector $\mathbf{r} = [r[0], r[1], \ldots r[N-1]]^T$, where $r[n] = r(n\Delta t)$. We assume that the CP is long enough to accommodate both the maximum TO and the channel delay spread, and thus there is no influence from the adjacent transmitted OFDM symbols.

A. Single-FFT receiver

In conventional single-FFT receiver, one FFT block is used to demodulate all users at the same time. The output of the single-FFT corresponding to the u^{th} user can be written in matricial form as

follows [2], [9]:

$$\mathbf{Z}_u = \mathbf{S}_u \mathbf{F}_N \mathbf{r} = \mathbf{S}_u \left(\mathbf{C}^p_{(\epsilon f_u)} \mathbf{Y}_u + \mathbf{C}^s_{(\epsilon f_u)} \mathbf{Y}_u + \sum_{u_1=0; u_1 \neq u}^{U-1} \mathbf{C}_{(\epsilon f_{u_1})} \mathbf{Y}_{u_1} + \mathbf{V} \right) \tag{5}$$

in which $\mathbf{F}_N$ stands for the size-N FFT matrix with entries $\mathbf{F}_N[n,k] = e^{-j2\pi nk/N}/\sqrt{N}$; $\mathbf{Z}_u = [Z_u[0], Z_u[1], \ldots Z_u[N-1]]^T$ and $\mathbf{V} = [V[0], V[1], \ldots V[N-1]]^T$, where $Z_u[k]$ and $V[k]$ are the u^{th} user's observed information and the AWGN contribution at the k^{th} subcarriers, respectively. $\mathbf{Y}_u = \mathbf{H}_u \mathbf{X}_u = [Y_u[0], Y_u[1], \ldots Y_u[N-1]]^T$ is the received signal from the u^{th} user without the effects of CFO. $\mathbf{H}_u$ is diagonal matrix of size N, whose the k^{th} non-zero diagonal entry, $H_u[k,k] = e^{-j2\pi \frac{k}{N} \epsilon t_u} \sum_{l=0}^{L-1} h_{u,l} e^{-j2\pi \frac{k}{T_o} \tau_{u,l}}$ for all $k \in \Delta_u$, is the Channel Transfer Function (CTF) at the k^{th} subcarrier of the u^{th} user. $\mathbf{X}_u = [X_u[0], X_u[1], \ldots X_u[N-1]]^T$ is the u^{th} user's transmitted symbol vector. $\epsilon t_u = \delta t_u / \Delta t$ and $\epsilon f_u = \delta f_u / \Delta f$ are the normalized TO and CFO of the u^{th} user. $\mathbf{S}_u$ is a diagonal matrix of size N, acting as a filter to select only subcarriers belonging to the u^{th} user, i.e. $\mathbf{S}_u(k,k) = 1$ for $k \in \Delta_u$, and all other diagonal elements are zero.

The $N \times N$ matrix $\mathbf{C}_{(\phi)}$ represents the shift due to the normalized CFO ϕ in frequency-domain. It is a circulant matrix respresenting the circular convolution operation:

$$\mathbf{C}_{(\phi)} = \mathbf{F}_N \mathbf{c}_{(\phi)} \mathbf{F}_N^H = \begin{bmatrix} \mathcal{C}(\phi) & \mathcal{C}(1+\phi) & \ldots & \mathcal{C}(N-1+\phi) \\ \mathcal{C}(N-1+\phi) & \mathcal{C}(\phi) & \ldots & \mathcal{C}(N-2+\phi) \\ \vdots & \vdots & \ddots & \vdots \\ \mathcal{C}(1+\phi) & \mathcal{C}(2+\phi) & \ldots & \mathcal{C}(\phi) \end{bmatrix} \tag{6}$$

where $\mathcal{C}(\phi) = \frac{\sin \pi\phi}{N \sin \pi\phi/N} e^{j\pi\phi(N-1)/N}$ is the periodic sinc-function [16], $[.]^H$ in the superscript denotes the Hermitian transpose operation, and $\mathbf{c}_{(\phi)}$ is a diagonal matrix of size N representing the CFO in time-domain, whose the n^{th} diagonal element is equal to $e^{j2\pi \frac{n}{N}\phi}$. The size N diagonal matrix $\mathbf{C}^p_{(\phi)}$ takes the principal diagonal entries of $\mathbf{C}_{(\phi)}$, while $\mathbf{C}^s_{(\phi)} = \mathbf{C}_{(\phi)} - \mathbf{C}^p_{(\phi)}$.

In the uplink of an OFDMA system with non-zero CFOs, the first term in (5) indicates an attenuation of the received signal, since $|\mathcal{C}(\epsilon f_u)|$ is always less than one if ϵf_u is non-zero. The second term represents the ICI among subcarriers of the same user, which is referred to as self-interference. And the third term is the cross-interference, which is the ICI among active users operating in the uplink. It is important to note that the conventional single-FFT receiver is not effective in multiple CFOs scenario, as it can be aligned to only one user at a given time, and the rest are mis-aligned [3].

B. The FD-MUIC receiver

In [17], the Choi-Lee-Jung-Lee (CLJL) scheme is proposed as an extension to the single-FFT receiver, which allows CFO correction after the FFT using circular convolution. The output of the

CLJL demodulator can be expressed as:

$$\begin{aligned}\mathbf{Z}_u^{\mathrm{CLJL}} &= \mathbf{S}_u\mathbf{C}_{(-\epsilon f_u)}\mathbf{Z}_u \\ &= \mathbf{S}_u\left(\mathbf{C}_{(-\epsilon f_u)}\mathbf{S}_u\mathbf{C}_{(\epsilon f_u)}\mathbf{Y}_u + \sum_{u_1=0;u_1\neq u}^{U-1}\mathbf{C}_{(-\epsilon f_u)}\mathbf{S}_u\mathbf{C}_{(\epsilon f_{u_1})}\mathbf{Y}_{u_1} + \mathbf{C}_{(-\epsilon f_u)}\mathbf{S}_u\mathbf{V}\right) \end{aligned} \quad (7)$$

where $\mathbf{C}_{(-\epsilon f_u)}$ represents the frequency-domain CFO correction by $-\epsilon f_u$. In [9], the Carrier to Interference-plus-Noise Ratio (CINR) analysis for CLJL scheme is given as follows:

$$\mathrm{CINR}_{u,k}^{\mathrm{CLJL}} = \frac{\sigma_{H_u}^2\sigma_{X_u}^2\left|\sum_{k_1\in\Delta_u}\mathcal{C}^2(k_1-k-\epsilon f_u)\right|^2}{\sigma_{I_{u,\mathrm{self}}^{\mathrm{CLJL}}[k]}^2 + \sigma_{I_{u,\mathrm{cross}}^{\mathrm{CLJL}}[k]}^2 + N_o} \quad (8)$$

$$\sigma_{I_{u,\mathrm{self}}^{\mathrm{CLJL}}[k]}^2 = \sigma_{H_u}^2\sigma_{X_u}^2\sum_{k_2\in\Delta_u;k_2\neq k}\left|\sum_{k_1\in\Delta_u}\mathcal{C}(k_2-k_1+\epsilon f_u)\mathcal{C}(k_1-k-\epsilon f_u)\right|^2 \quad (9)$$

$$\sigma_{I_{u,\mathrm{cross}}^{\mathrm{CLJL}}[k]}^2 = \sum_{u_1=0;u_1\neq u}^{U-1}\sigma_{H_{u_1}}^2\sigma_{X_{u_1}}^2\sum_{k_2\in\Delta_{u_1}}\left|\sum_{k_1\in\Delta_u}\mathcal{C}(k_2-k_1+\epsilon f_{u_1})\mathcal{C}(k_1-k-\epsilon f_u)\right|^2 \quad (10)$$

where $\sigma_{H_u}^2 = E[|H_u|^2]$ is the average gain of the u^{th} user's channel, and $N_o/2$ is the power spectral density of the AWGN. (8) shows that, when the CFO is large, the CLJL scheme suffers from attenuation of the signal of interest, due to the fact that signal power does not concentrate in the prescribed subcarrier positions [9]. In addition, there exists residual self- and cross-interference terms, which cause the degradation of the system performance. The FD-MUIC scheme proposed in [9] is a Parallel Interference Cancellation (PIC) scheme, which aims at removing the cross-interference. The output of the FD-MUIC demodulator at the i^{th} iteration is given by:

$$\begin{aligned}\mathbf{Z}_{u,i}^{\mathrm{FD-MUIC}} &= \mathbf{Z}_u^{\mathrm{CLJL}} - \sum_{u_1=0;u_1\neq u}^{U-1}\mathbf{S}_u\mathbf{C}_{(-\epsilon f_u)}\mathbf{S}_u\mathbf{C}_{(\epsilon f_{u_1})}\mathbf{Z}_{u_1,i-1}^{\mathrm{FD-MUIC}} \\ &= \mathbf{S}_u\left(\mathbf{C}_{(-\epsilon f_u)}\mathbf{S}_u\mathbf{C}_{(\epsilon f_u)}\mathbf{Y}_u + \sum_{u_1=0;u_1\neq u}^{U-1}\mathbf{C}_{(-\epsilon f_u)}\mathbf{S}_u\mathbf{C}_{(\epsilon f_{u_1})}\left(\mathbf{Y}_{u_1} - \mathbf{Z}_{u_1,i-1}^{\mathrm{FD-MUIC}}\right)\right. \\ &\quad \left.+\mathbf{C}_{(-\epsilon f_u)}\mathbf{S}_u\mathbf{V}\right) \end{aligned} \quad (11)$$

and $\mathbf{Z}_{u,0}^{\mathrm{FD-MUIC}} = \mathbf{Z}_u^{\mathrm{CLJL}}$. Since the CINR analysis for FD-MUIC scheme in [9] does not account for the fact that the signal of interest is attenuated with non-zero CFO, hence a closer approximation of CINR is introduced here:

$$\mathrm{CINR}_{u,k,i}^{\mathrm{FD-MUIC}} = \frac{\sigma_{H_u}^2\sigma_{X_u}^2\left|\sum_{k_1\in\Delta_u}\mathcal{C}^2(k_1-k-\epsilon f_u)\right|^2}{\sigma_{I_{u,\mathrm{self}}^{\mathrm{CLJL}}[k]}^2 + \sigma_{I_{u,\mathrm{cross},i}^{\mathrm{FD-MUIC}}[k]}^2 + N_o} \quad (12)$$

$$\sigma^2_{I^{\text{FD-MUIC}}_{u,\text{cross},i}[k]} \approx \sum_{u_1=0;u_1\neq u}^{U-1} \sum_{k_2\in\Delta_{u_1}} \left(\sigma^2_{H_{u_1}}\sigma^2_{X_{u_1}} \left(1 - \left| \sum_{k_3\in\Delta_{u_1}} \mathcal{C}^2(k_3-k_2-\epsilon f_{u_1}) \right| \right)^2 + \sigma^2_{I^{\text{CLJL}}_{u_1,\text{self}}[k_2]} + \sigma^2_{I^{\text{FD-MUIC}}_{u_1,cross,i-1}[k_2]} + N_o \right) \left| \sum_{k_1\in\Delta_u} \mathcal{C}(k_2-k_1+\epsilon f_{u_1})\mathcal{C}(k_1-k-\epsilon f_u) \right|^2$$

$$\text{for } i >= 1 \tag{13}$$

where $\sigma^2_{I^{\text{FD-MUIC}}_{u,\text{cross},0}[k]} = \sigma^2_{I^{\text{CLJL}}_{u,\text{cross}}[k]}$.

To provide comparable results with [9], we consider the same OFDMA uplink system, where the number of user is $U = 4$. Each user is allocated 16 subcarriers ($N = 64$), and the CFOs are $\epsilon f_1 = 0.10$, $\epsilon f_2 = -0.10$, $\epsilon f_3 = -0.05$ and $\epsilon f_4 = 0.05$, respectively. Two subcarrier allocation schemes are considered: Block- and interleaved-allocation. In block allocation, the spectrum is uniformly divided into U blocks, where each user is assigned one block. In interleaved allocation, the subcarriers are uniformly interleaved across all the users. The CNR is 40dB, and we assume perfect CFO knowledge at the receiver. In Fig. 1, the average CINR performance of the FD-MUIC scheme is plotted against the number of iterations. The average CINR is computed by averaging the CINR at all subcarrier from all users. Two methods of CINR analysis are compared to simulation results: Huang-Letaief (HL) refers to the analysis provided in [9], while Nguyen-Carvalho-Prasad (NCP) refers to equation (12). Both methods are named after their authors. It can be seen that our method provides much closer approximation, since the power loss due to filtering process has been taken into account. It is also worthy to note that, in FD-MUIC scheme, the interleaved allocation outperforms the block after few iterations. This is due to the fact that self-interference term, which cannot be removed by FD-MUIC scheme, is smaller in the case of interleave allocation, compared to the block case.

C. CTYH receiver

The CTYH receiver is based on a single-FFT receiver, which aims at reconstructing the orthogonality among users in frequency-domain [2]. This goal is obtained by means of a linear transformation applied to:

$$\mathbf{Z} = \sum_{u=0}^{U-1} \mathbf{Z}_u = \mathbf{\Pi H X} + \mathbf{V} \tag{14}$$

where $\mathbf{Z}_u$ is defined in (5), $\mathbf{\Pi} = \sum_{u=0}^{U-1} \mathbf{C}_{(\epsilon f_u)}\mathbf{S}_u$ is the $N \times N$ interference matrix, $\mathbf{H} = \sum_{u=0}^{U-1} \mathbf{H}_u$ is CTF matrix and $\mathbf{X} = \sum_{u=0}^{U-1} \mathbf{X}_u$ is the transmitted symbol vector. The linear unbiased Minimum Mean Square Error (MMSE) estimator [18] is chosen for performance comparison in section III-A. The output CINR of the linear unbiased MMSE estimator at the k^{th} subcarrier is given by [18], [19]:

$$\mathrm{CINR}_{MMSE,k}^{\mathrm{CTYH}} = \frac{\sigma_X^2}{\left[(\mathbf{H}^H\mathbf{\Pi}^H\mathbf{\Pi}\mathbf{H} + \frac{N_o}{\sigma_X^2}\mathbf{I})^{-1}N_o\right]_{kk}} - 1 \quad (15)$$

where all users transmit with equal power (i.e. $\sigma_{X_u}^2 = \sigma_X^2$ for all u) and $[.]_{kk}$ denotes the k^{th} diagonal element. It is worth noting that the CTYH receiver cannot achieve CFO-free performance, because it is based on a linear transformation technique.

D. Multi-FFT receiver

In multi-FFT receiver structure, each active user is assigned one OFDM-demodulator block, so that their CFOs can be compensated for independently in the time-domain. After CFO compensation, the output of the OFDM demodulator belonging to the u^{th} user can be expressed as [20]:

$$\mathbf{Z}_u^{\mathrm{mFFT}} = \mathbf{S}_u\mathbf{F}_N\mathbf{c}_{(-\epsilon f_u)}\mathbf{r} = \mathbf{S}_u\left(\mathbf{Y}_u + \sum_{u_1=0;u_1\neq u}^{U-1}\mathbf{C}_{(\epsilon f_{u_1-u}^{\mathrm{mFFT}})}\mathbf{Y}_{u_1} + \mathbf{C}_{(-\epsilon f_u)}\mathbf{V}\right) \quad (16)$$

where $\mathbf{c}_{(-\epsilon f_u)}$ represents the time-domain CFO correction by $-\epsilon f_u$, and $[.]^{\mathrm{mFFT}}$ in superscript refers to the fact that multiple FFT blocks are employed. $\epsilon f_{u_1-u}^{\mathrm{mFFT}} = \epsilon f_{u_1} - \epsilon f_u$ denotes the relative CFO between the u^{th} and u_1^{th} user. (5) and (16) show that, by using the multi-FFT receiver, the attenuation factor and the self-interference have disappeared for the desired u^{th} user, provided that its CFO, ϵf_u, is estimated correctly. However, the cross-interference term is still present, and can sometimes become larger due to the fact that the new CFO, $\epsilon f_{u_1-u}^{\mathrm{mFFT}}$, might be larger than the original one, ϵf_{u_1}. This tends to cause significant performance degradation [17], and the aim of the this paper is to further remove such interference to achieve the CFO-free performance.

III. Our proposals

(16) indicates that the cross-interference term is a deterministic function, which depends on the transmitted data symbols, the channel frequency responses, the TOs and CFOs of all other active users in the OFDMA system. In the case of cellular's uplink, these parameters are estimated by, and therefore, available to the BS, which inspires the idea of applying the principle of multiuser interference cancellation. In this section, two MUI receiver structures are proposed for the OFDMA uplink, namely Simple Time-Domain Multi-User Interference Cancellation Scheme (SI-MUIC) and Code-Aided Time-Domain Multi-User Interference Cancellation Scheme (CA-MUIC). They are both based on the multi-FFT receiver, as illustrated in Fig. 3, and their algorithms are explained as follows:

A. The SI-MUIC scheme

Assume that users are sorted in order of their Received Signal Strengths (RSSs), and the BS processes from the user with the strongest received power to the one with lowest power, thus increases the chance of correct estimation and decoding. The iterative Successive Interference Cancellation (SIC) implementation of SI-MUIC scheme can be shown as following:

SI-MUIC's SIC Algorithm

Initialization: Set $i = 0$

$$\hat{\mathbf{r}}_{u,i}^{\mathrm{SI-MUIC}} = 0 \text{ for } u = 0, 1, \ldots U-1 \tag{17}$$

Loop A: $i = i + 1$ and $u = 0$

Loop B:

$$\mathbf{Z}_{u,i}^{\mathrm{SI-MUIC}} = \mathbf{S}_u \mathbf{F}_N \mathbf{c}_{(\epsilon f_u)} \left(\mathbf{r} - \sum_{u_1=0}^{u-1} \hat{\mathbf{r}}_{u_1,i}^{\mathrm{SI-MUIC}} - \sum_{u_2=u+1}^{U-1} \hat{\mathbf{r}}_{u_2,i-1}^{\mathrm{SI-MUIC}} \right) \tag{18}$$

$$\hat{\mathbf{r}}_{u,i}^{\mathrm{SI-MUIC}} = \mathbf{c}_{(-\epsilon f_u)} \mathbf{F}_N^H \mathbf{Z}_{u,i}^{\mathrm{SI-MUIC}} \tag{19}$$

$u = u + 1$

Go to Loop B until $u > U - 1$

Go to Loop A until $i > N_{loop}$

In the algorithm, $\hat{\mathbf{r}}_{u,i}^{\mathrm{SI-MUIC}}$ denotes the feedback signal from the u^{th} user at the i^{th} step. The demodulation and calculation of the feedback signal in the SI-MUIC scheme is illustrated in Fig 4. (18) can be re-written as:

$$\mathbf{Z}_{u,i}^{\mathrm{SI-MUIC}} = \mathbf{S}_u \left(\mathbf{Y}_u + \sum_{u_1=0}^{u-1} \mathbf{C}_{(\epsilon f_{u_1-u}^{\mathrm{mFFT}})} \mathbf{I}_{u_1,i}^{\mathrm{SI-MUIC}} + \sum_{u_2=u+1}^{U-1} \mathbf{C}_{(\epsilon f_{u_2-u}^{\mathrm{mFFT}})} \mathbf{I}_{u_2,i-1}^{\mathrm{SI-MUIC}} + \mathbf{C}_{(-\epsilon f_u)} \mathbf{V} \right) \tag{20}$$

$$\mathbf{I}_{u,i}^{\mathrm{SI-MUIC}} = \begin{cases} \mathbf{Y}_u & i = 0 \\ \mathbf{Y}_u - \mathbf{S}_u \mathbf{Z}_{u,i}^{\mathrm{SI-MUIC}} & i > 0 \end{cases} \tag{21}$$

where $\mathbf{I}_{u,i}^{\mathrm{SI-MUIC}}$ is the residual estimation error after the i^{th} iteration. (16) and (20) are identical, except that, for $i > 0$, the received signal $\mathbf{Y}_{u_1}$ has been replaced by the estimation error, $\mathbf{I}_{u_1,i}^{\mathrm{SI-MUIC}}$ or $\mathbf{I}_{u_2,i-1}^{\mathrm{SI-MUIC}}$. This indicates the gain from using the SI-MUIC scheme: The cross-interference term shall be reduced, provided that the estimation error for the u^{th} user is small, or $\mathbf{S}_u \mathbf{Z}_{u,i}^{\mathrm{SI-MUIC}}$ is a good estimate of $\mathbf{Y}_u$. We observe that the estimation error at the i^{th} iteration is the sum of the other users' estimation errors from current or previous iteration, attenuated by a periodic sinc function, $\mathbf{C}_{(\epsilon f_{u_1-u}^{\mathrm{mFFT}})}$

or $\mathbf{C}_{(\epsilon f_{u_2-u}^{\mathrm{mFFT}})}$, respectively. In general, thanks to this attenuation, the estimation error is reduced with the increased number of iterations, which is shown afterwards by numerical evaluation.

Fig. 2 illustrates the convergence property of the SIC implementation of the SI-MUIC scheme, under the same OFDMA system's setting as in section II-B, where $U = 4$, $N = 64$ and the CFOs are fixed. The PIC implementation of the SI-MUIC, which is similar to the one described in [9] and section II-B, is also included for comparison. The output of the OFDMA demodulator in case of PIC implementation for the u^{th} user at the i^{th} iteration is given by:

$$\mathbf{Z}_{u,i}^{\mathrm{SI-MUIC,PIC}} = \mathbf{S}_u \left(\mathbf{Y}_u + \sum_{u_1=0; u_1 \neq u}^{U-1} \mathbf{C}_{(\epsilon f_{u_1-u}^{\mathrm{mFFT}})} \mathbf{I}_{u_1,i-1}^{\mathrm{SI-MUIC,PIC}} + \mathbf{C}_{(-\epsilon f_u)} \mathbf{V} \right) \tag{22}$$

$$\mathbf{I}_{u,i}^{\mathrm{SI-MUIC,PIC}} = \begin{cases} \mathbf{Y}_u & i = 0 \\ \mathbf{Y}_u - \mathbf{S}_u \mathbf{Z}_{u,i}^{\mathrm{SI-MUIC,PIC}} & i > 0 \end{cases} \tag{23}$$

Firstly, Fig. 2 shows that the performance of the SIC implementation is always superior than those of the PIC, for both FD-MUIC and SI-MUIC, even at the iteration $i = 0$. This can be explained by looking at (20) and (22): PIC only utilizes the estimations from the previous iteration, whereas in SIC the estimation of the u^{th} user is done based on current estimates $\mathbf{S}_{u_1} \mathbf{Z}_{u_1,i}^{\mathrm{SI-MUIC}}$ of the u_1^{th} users ($u_1 < u$). Since these new estimates are with less interference, the performance of SIC is always superior compared to PIC. Nevertheless, the SIC is penalized with a longer delay than PIC, since the last user can only be processed when all the others have been demodulated. Secondly, as more iterations are performed, the FD-MUIC schemes quickly come to an irreducible noise floor, due to the fact that the power loss and the self-interference term remain unchanged, compared to the CLJL scheme. The SI-MUIC scheme does not have such an irreducible noise floor. The CFO-free performance can be achieved after 4 iterations. The performance of the CTYH scheme is also plotted in Fig. 2 for comparison.

It is worth noting that the SI-MUIC scheme does not require Channel State Information (CSI), all it needs to know is the CFO value of each user. The residual noise and interference term in SI-MUIC can be further removed, which is the aim of the CA-MUIC explained in the next section.

B. The CA-MUIC scheme

The main different between CA-MUIC and SI-MUIC scheme is that, instead of the output of the OFDMA demodulator $\mathbf{Z}_{u,i}^{\mathrm{SI-MUIC}}$, the estimation $\hat{\mathbf{Y}}_{u,i}$ is used to calculate the feedback.

CA-MUIC's SIC Algorithm

Initialization: Set $i = 0$

$$\hat{\mathbf{r}}_{u,i}^{\mathrm{CA-MUIC}} = 0 \text{ for } u = 0, 1, \ldots U-1 \tag{24}$$

Loop A: $i = i + 1$ and $u = 0$

Loop B:

$$\mathbf{Z}_{u,i}^{\mathrm{CA-MUIC}} = \mathbf{S}_u \mathbf{F}_N \mathbf{c}_{(\epsilon f_u)} \left(\mathbf{r} - \sum_{u_1=0}^{u-1} \hat{\mathbf{r}}_{u_1,i}^{\mathrm{CA-MUIC}} - \sum_{u_2=u+1}^{U-1} \hat{\mathbf{r}}_{u_2,i-1}^{\mathrm{CA-MUIC}} \right) \tag{25}$$

Estimate $\hat{\mathbf{Y}}_{u,i}$ from $\mathbf{Z}_{u,i}^{\mathrm{CA-MUIC}}$.

$$\hat{\mathbf{r}}_{u,i}^{\mathrm{CA-MUIC}} = \mathbf{c}_{(-\epsilon f_u)} \mathbf{F}_N^H \hat{\mathbf{Y}}_{u,i} \tag{26}$$

$u = u + 1$

Go to Loop B until $u > U - 1$

Go to Loop A until $i > N_{loop}$

Fig 5 shows the demodulation block for CA-MUIC scheme. Similar to the SI-MUIC scheme, (25) can be re-written as:

$$\mathbf{Z}_{u,i}^{\mathrm{CA-MUIC}} = \mathbf{S}_u \left(\mathbf{Y}_u + \sum_{u_1=0}^{u-1} \mathbf{C}_{(\epsilon f_{u_1-u}^{\mathrm{mFFT}})} \mathbf{I}_{u_1,i}^{\mathrm{CA-MUIC}} + \sum_{u_2=u+1}^{U-1} \mathbf{C}_{(\epsilon f_{u_2-u}^{\mathrm{mFFT}})} \mathbf{I}_{u_2,i-1}^{\mathrm{CA-MUIC}} + \mathbf{C}_{(-\epsilon f_u)} \mathbf{V} \right) \tag{27}$$

$$\mathbf{I}_{u,i}^{\mathrm{CA-MUIC}} = \begin{cases} \mathbf{Y}_u & i = 0 \\ \mathbf{Y}_u - \mathbf{S}_u \hat{\mathbf{Y}}_{u,i} & i > 0 \end{cases} \tag{28}$$

And the output of the CA-MUIC demodulator in case of the PIC implementation is given by:

$$\mathbf{Z}_{u,i}^{\mathrm{CA-MUIC,PIC}} = \mathbf{S}_u \left(\mathbf{Y}_u + \sum_{u_1=0; u_1 \neq u}^{U-1} \mathbf{C}_{(\epsilon f_{u_1-u}^{\mathrm{mFFT}})} \mathbf{I}_{u_1,i-1}^{\mathrm{CA-MUIC,PIC}} + \mathbf{C}_{(-\epsilon f_u)} \mathbf{V} \right) \tag{29}$$

$$\mathbf{I}_{u,i}^{\mathrm{CA-MUIC,PIC}} = \begin{cases} \mathbf{Y}_u & i = 0 \\ \mathbf{Y}_u - \mathbf{S}_u \hat{\mathbf{Y}}_{u,i}^{\mathrm{PIC}} & i > 0 \end{cases} \tag{30}$$

where $\hat{\mathbf{Y}}_{u,i}^{\mathrm{PIC}}$ is estimated from $\mathbf{Z}_{u,i}^{\mathrm{CA-MUIC,PIC}}$. It is important to note that the task of estimating $\hat{\mathbf{Y}}_{u,i}$ and $\hat{\mathbf{Y}}_{u,i}^{\mathrm{PIC}}$ in the CA-MUIC algorithm is actually boiled down to estimating the CTF, $\hat{H}_{u,i}[k]$, and the transmitted data symbol, $\hat{X}_{u,i}[k]$, for the u^{th} user. If such estimations are correct, the second term in (27) will go to zero, leaving no cross-interference at the output of the u^{th} user's OFDMA demodulator. In order to achieve correct estimation of the data symbols, channel coding is applied in the CA-MUIC scheme, hence it is referred to as code-aided TD-MUIC scheme.

C. Computational complexity

The SI-MUIC scheme requires two FFT operations for each user in each iteration, one for demodulation and another for regenerating the corresponding time-domain signal. Therefore, the computation complexity of the SI-MUIC scheme is $\mathrm{O}(2UN_{loop}N\log_2 N)$, where $\mathrm{O}(.)$ and N_{loop} denote the order of complexity and number of iterations, respectively. Note that the SIC and PIC implementations are equivalent on complexity, as they require the same number of FFT operations per user per loop. The complexity of CA-MUIC scheme is larger than SI-MUIC, as decoding/coding, symbol demapping/mapping and channel insertion are involved. CA-MUIC's complexity is not accounted for in this paper, as it is considered only as an enhancement to SI-MUIC.

The FD-MUIC needs only one FFT operation at the beginning, but it requires U circular convolutions for each user in each iteration. The complexity of circular convolution can be reduced by considering only $P-1$ out of $N-1$ most dominant interfering subcarriers, at the cost of performance degradation [9]. The computation complexity of the FD-MUIC scheme in that case is $\mathrm{O}(UN_{loop}NP)$ [12], without considering the complexity of constructing the CFO correction matrices $\mathbf{C}_{(-\epsilon f_u)}$. Constructing CFO correction matrices requires computation of periodic sinc-function $\mathcal{C}(\phi)$, which can be costly and subjected to fixed-point precision problem. The CTYH scheme does not depend on the number of users and the number of iterations, but in principle it cost $\mathrm{O}(N^3)$ due to matrix inversion [12]. The complexity of the CTYH scheme can also be reduced by considering only $P-1$ most dominant interfering subcarriers, but the trade-off is performance degradation. Table I shows the number of arithmetic operations required for SI-MUIC, FD-MUIC and CTYH for different number of FFT size, where $U=10$ and $N_{loop}=5$. The complexity of the SI-MUIC is comparable to that of the FD-MUIC with $P=25$, while its performance exceeds that of the FD-MUIC with $P=N$.

IV. Numerical Evaluation

A. CFO estimation

In the previous section, the performance of the proposed schemes has been analyzed under assumption of perfect CFO knowledge. In this section, we demonstrate the feasibility of the proposed schemes by using a realistic CFO estimation technique.

To assist CFO estimation during data transmission, pilot subcarriers are inserted repeatedly in the first two OFDMA symbols by all active users. Let Δ_u^p denote the indexes of pilot subcarriers for the u^{th} user, and $Z_{u,1}=\{z_{u,1,p}, p\in\Delta_u^p\}$ and $Z_{u,2}=\{z_{u,2,p}, p\in\Delta_u^p\}$ are the sets of pilot subcarriers transmitted at the first and the second symbol, respectively. The Maximum Likelihood (ML) estimate

of the CFO $\hat{\epsilon f}_u$, given the observations $Z_{u,1}$ and $Z_{u,2}$, is the value of $\hat{\epsilon f}_u$ that maximizes the conditional joint density function of the observations:

$$\hat{\epsilon f}_u = \max_{\hat{\epsilon f}_u} [f(Z_{u,1}, Z_{u,2} | \hat{\epsilon f}_u)] \tag{31}$$

The result of this estimate is given by [14]

$$\hat{\epsilon f}_u = \frac{1}{2\pi} \tan^{-1} \frac{\sum_{p \in \Delta_u^p} \mathrm{Im}(z_{u,2,p} z_{u,1,p}^*)}{\sum_{p \in \Delta_u^p} \mathrm{Re}(z_{u,2,p} z_{u,1,p}^*)} \tag{32}$$

where $\tan^{-1}$ is the arctangent function, and $\mathrm{Im}(.)$ and $\mathrm{Re}(.)$ are imaginary and real part of the complex value, respectively. The limit of this estimator is half of the subcarrier spacing. Therefore, prior to uplink data transmission, a coarse frequency synchronization must be performed, for example using estimation techniques described in [13], [14] or via the initial or periodic ranging procedures stated in IEEE 802.16 standard [15], to bring the CFO down to tolerable value.

B. Simulation results

Unless otherwise stated, the basic simulation parameters are taken from Table II. Thanks to a coarse synchronization stage, the TOs of all users are well within the CP and the CFOs are less than the maximum torelable value of the system, ϵf_{max}. We assume the received powers of all active users are equal and the CTF is perfectly estimated. Note that the CTF information is only required for CA-MUIC, not SI-MUIC. There are 5 users in the system, and at each transmission they experiences a CFO between $[-\epsilon f_{max}, +\epsilon f_{max}]$. Both block and interleaved subcarrier allocation schemes are used for evaluation, and there is no guardband between users in frequency domain. Only SIC implementation is evaluated for the sake of simplicity.

Fig. 6 shows the uncoded Bit Error Rate (BER) performance of the proposed schemes with different maximum CFO values. While the performance of the single-FFT receiver drops dramatically with the increase of the maximum CFOs value, both the SI-MUIC and CA-MUIC schemes can tolerate up to 10% of subcarrier spacing with little degradation. Especially in block allocation setting, the CA-MUIC scheme can achieve offset-free performance with up to 40% of subcarrier spacing.

For a fair comparison, the performance of FD-MUIC is only compared to that of the SI-MUIC, which also does not utilize channel coding. In general, the SI-MUIC extends the maximum torelable CFO by about 5% of subcarrier spacing, compared to the FD-MUIC. This is due to the fact that the SI-MUIC can avoid the power loss and the self-interference problems occurring in the FD-MUIC scheme. Negligible performance degradation is observed for most of the discussed IC schemes when $\epsilon f_{max} = 0.25$, therefore we will hereafter use this value.

Fig. 7 shows the convergence properties of the CA-MUIC scheme, plotted along with the SIC implementation of FD-MUIC and SI-MUIC. In case of block allocation, the CA-MUIC converges faster than SI-MUIC, achieving the CFO-free performance in only two iterations. In interleaved allocation setting, it converges much slower than the SI-MUIC scheme. The main source of performance degradation in this case is the error propagation phenomenon: the applied convolutional code is not strong enough to overcome large MUI from neighboring users, thus produce bit errors in detection, and those errors propagate from one iteration to the others. A stronger code is required to achieve better performance in interleaved subcarrier allocation scenario, or alternatively, the SI-MUIC can be applied in the first few iterations to clean up the received signal to a level which the the CA-MUIC scheme can work effectively. Similar to SI-MUIC, the PIC implementation of the CA-MUIC scheme performs worse than its SIC version.

The uncoded BER performance versus CNR is shown in the Fig. 8. In the single-FFT receiver, the self- and cross-interference causes an irreducible error floor, which cannot be overcome by increasing the transmit power. This error floor is brought down by applying IC schemes, such as FD-MUIC, SI-MUIC or CA-MUIC. The SI-MUIC scheme shows considerable performance gain compared to the FD-MUIC, in both block and interleaved subcarrier allocation scenarios. And CFO-free performance can be achieved with CA-MUIC in block subcarrier allocation scenario.

Fig. 9 illustrates the uncoded BER performance for different numbers of users. All available subcarriers are divided equally among users using both block and interleaved allocation schemes. The number of iterations is kept constant with the increase of the number of users (i.e. $N_{loop} = 5$). We observe that the single-FFT receiver works well when there is only one user, while the IC schemes can accommodate more users, each of which experiences an independent CFOs value. Again, the SI-MUIC shows much better performance than the FD-MUIC: the uncoded BER deteriorates much slower with the increase of the system load. Unlike in Code Division Multiple Access (CDMA) technique, the MUI in OFDMA does not increase linearly with the number of users, since the MUI caused by one subcarrier to another subcarrier decreases quickly as the distance between these two subcarriers increases [2]. Therefore, the performance of the SI-MUIC scheme is expected to change insignificantly when the number of users becomes greater than 10. In the block subcarrier allocation, the CA-MUIC achieves CFO-free performance even at 10 users. On the contrary, the CA-MUIC performs poorly in interleaved subcarrier allocation scheme, especially when there are only two users. This is due to the fact that all MUI to a subcarrrier of the first user are coming from the second user, and vice versa. If the relative CFO between them is large, the system performance will experience great impact due to the error propagation phenomena. When the number of users increases, the MUI to a subcarrier of a user comes from several adjacent users, and the probability that all relative CFOs are simultaneously

large is small, therefore we can observe some performance gain.

Due to the limited space of the paper, we consider that each user is allocated the same number of subcarriers. However, the SI-MUIC scheme works well in any subcarrier allocation schemes, provided that the CFO estimates of users are available. The number of subcarriers dictates the coding length and the coding diversity for the CA-MUIC scheme, therefore too few subcarriers allocated to a user can cause its performance to degrade. It is also worth noting that the interleaved subcarrier allocation scheme analyzed in this paper is considered as the worst case scenario for all the other allocation schemes.

V. Conclusions

This paper has proposed novel MUI cancellation schemes, which are very effective against the effects of multiple CFOs scenario in the uplink OFDMA. Analytical and numerical evaluation has shown that the schemes outperform the performance of the conventional OFDMA receiver and the FD-MUIC scheme, for both block and interleaved subcarrier allocations. The proposed schemes are especially useful in scenarios where BS cannot instruct users to adjust their CFO or implementation of such instruction is expensive (e.g. there is no feedback channel or low cost terminal does not have ability to adjust its frequency base accurately). They are compatible with current standard for MS using OFDMA technique, for example IEEE 802.16, since all changes are transparent for MS. The proposed schemes introduce additional complexity, which can be justified by the fact that the complexity is added only to BS and the lower cost and faster operation of FFT processing chip. It worth noting that the complexity of the proposed schemes is comparable or lower than the existing frequency-domain MUI cancellation techniques in literature. The schemes show good performance under practical CFO estimator, and the performance converge after several iterations.

Acknowledgement

The authors would like to thank Samsung Electronics, Co. LTD, Korea for supporting this work.

References

[1] T. Pollet, M. van Bladel, and M. Moeneclaey, "BER sensitivity of OFDM systems to carrier frequency offset and Wiener phase noise," *IEEE Trans. Comm.*, vol. 43, no. 2/3/4, Feb/Mar/Apr 1995.

[2] Z. Cao, U. Tureli, Y.-D. Yao, and P. Honan, "Frequency Synchronization for Generalized OFDMA Uplink," in *IEEE Globecom*, November 2004.

[3] M. Morelli, "Timing and frequency synchronization for the uplink of and OFDMA system," *IEEE Transactions on Communications*, vol. 52, no. 2, February 2004.

[4] J.-J. van de Beek, P. O. Borjesson, M.-L. Boucheret, D. Landstrom, J. M. Arenas, P. Odling, C. Osterberg, M. Wahlqvist, and S. K. Wilson, "A time and frequenc synchronization scheme for multiuser OFDM," *IEEE Journal on Selected Areas in Communications*, vol. 17, no. 11, November 1999.

[5] M. Gudmundson and P.-O. Anderson, "Adjacent channel interference in an OFDM system," in *Vehicular Technology Conference, IEEE*, April 1996.

[6] C. Muschallik, "Improving an OFDM reception using an adaptive Nyquist windowing," *IEEE Transactions on Consumer Electronics*, vol. 42, August 1996.

[7] J. Armstrong, "Analysis of new and existing methods of reducing intercarrier interference due to carrier frequency offset in OFDM," *IEEE Transactions on Communications*, vol. 47, March 1999.

[8] Y. Zhao and S.-G. Haggman, "Intercarrier Interference Self-Cancellation Scheme for OFDM Mobile Communication Systems," *IEEE Transactions on Communications*, vol. 49, July 2001.

[9] D. Huang and K. B. Letaief, "An Interference-Cancellation Scheme for Carrier Frequency Offsets Correction in OFDMA Systems," *IEEE Transactions on Communications*, vol. 53, no. 7, July 2005.

[10] Z. Cao, U. Tureli, and Y.-D. Yao, "User Separation and Frequency-Time Synchronization for the Uplink of Interleaved OFDMA," in *IEEE Signals, Systems and Computers*, Pacific Grove, USA, November 2002.

[11] ——, "Deterministic multiuser carrier-frequency offset estimation for interleaved OFDMA uplink," *IEEE Transaction on Communications*, vol. 52, no. 9, September 2004.

[12] M. Morelli, C.-C. J. Kuo, and M.-O. Pun, "Synchronization Techniques for Orthogonal Frequency Division Multiple Access (OFDMA): A Tutorial Review," *Proceedings of the IEEE*, vol. 95, no. 7, pp. 1394–1427, July 2007.

[13] T. M. Schmidl and D. C. Cox, "Robust frequency and timing synchronization for OFDM," *IEEE Trans. Comm.*, December 1997.

[14] P. H. Moose, "A technique for orthogonal frequency division multiplexing frequency offset correction," *IEEE Trans. Comm.*, vol. 42, pp. 2908–2914, October 1994.

[15] IEEE LAN/MAN Standards Committee, "Part 16: Air interface for fixed broadband wireless access systems," *IEEE*, 2004.

[16] D. Galda, H. Rohling, and E. Costa, "On the effects of user mobility on the uplink an OFDMA system," in *IEEE VTC*, vol. 2, April 2003, pp. 1433–1437.

[17] J. Choi, C. Lee, H. W. Jung, and Y. H. Lee, "Carrier frequency offset compensation for uplink of ofdm-fdma systems," *IEEE Communications Letters*, vol. 4, pp. 414–416, December 2000.

[18] J. M. Cioffi, G. P. Dudevoir, M. V. Eyuboglu, and G. D. Forney, "MMSE Decision-Feedback Equalisers and Coding - Part I: Equalization Results," *IEEE Transactions on Communications*, vol. 43, no. 10, pp. 2582–2594, October 1995.

[19] D. Tse and P. Viswanath, *Fundamentals of Wireless Communications*. Cambridge Press, May 2005.

[20] H. C. Nguyen, E. de Carvalho, and R. Prasad, "Multi-user Interference Cancellation Scheme(s) for Multiple Carrier Frequency Offset Compensation in Uplink OFDMA," in *IEEE PIMRC*, Helsinki, Finland, September 2006.

[21] IEEE LAN/MAN Standards Committee, "Part 11: Wireless LAN Medium Access Control (MAC) and Physical Layer (PHY) specifications: High-speed Physical Layer in the 5 GHz Band," *IEEE*, 1999.

[22] R. Vaughan and J. B. Andersen, *Channels propagation and antennas for mobile communications*. IEE Electromagnetic Waves Series 50, 2003, no. ISBN 0-85296084-0.

TABLE I

NUMBER OF ARITHMETIC OPERATIONS (IN THOUSAND)

Scheme	N=1024	N=2048	N=4096
SI-MUIC	1.024	2.253	4.915
FD-MUIC (P=5)	256	512	1.024
FD-MUIC (P=15)	768	1.536	3.072
FD-MUIC (P=25)	1.028	2.560	5.120
FD-MUIC (P=N)	52.429	209.715	838.861
CTYH	1.073.742	8.589.935	68.719.477

TABLE II

SYSTEM PARAMETERS

Parameter	Value
System bandwidth	40MHz
Number of subcarriers	1024
CP length	400 samples
Subcarrier allocation scheme	Block and Interleaved
Modulation	Quadrature Phase Shift Keying (QPSK)
Channel coding/decoding	1/2 convolution code with Viterbi decoder [21]
Channel model	7-tap exponential decay Rayleigh fading channel [22]
Channel rms delay spread	1us
CNR	40dB
Number of users	5
Number of subcarriers per user	200
Number of iterations (N_{loop})	5

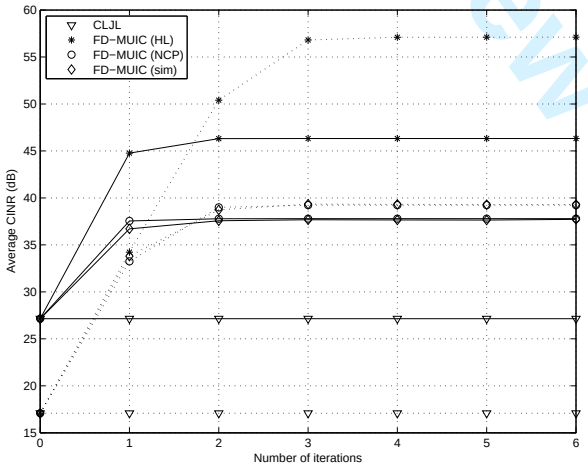

Fig. 1. Average CINR performance of the FD-MUIC scheme. Solid line indicates block allocation, and dotted line represents interleaved allocation.

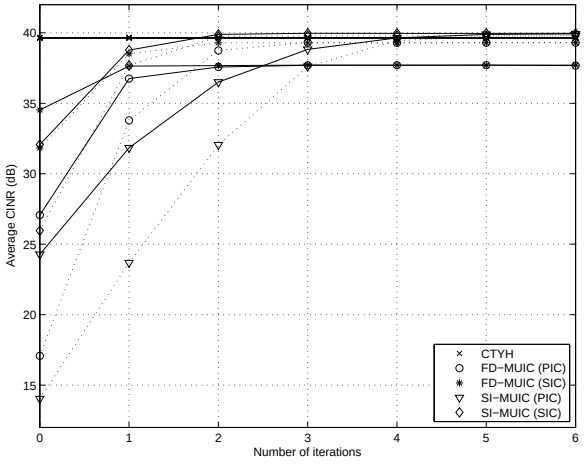

Fig. 2. Average CINR performance of the PIC and SIC implementations of the FD-MUIC and SI-MUIC schemes. Solid line indicates block allocation, and dotted line represents interleaved allocation.

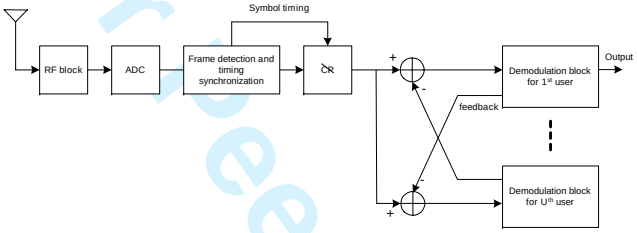

Fig. 3. General receiver structure for the Time-domain multi-user interference cancellation schemes

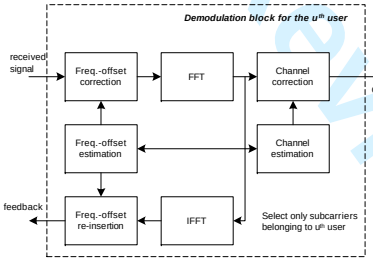

Fig. 4. Demodulation block for SI-MUIC scheme

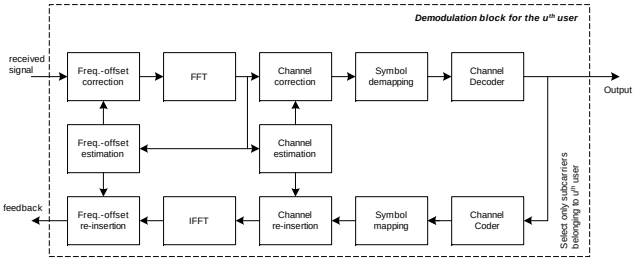

Fig. 5. Demodulation block for CA-MUIC scheme

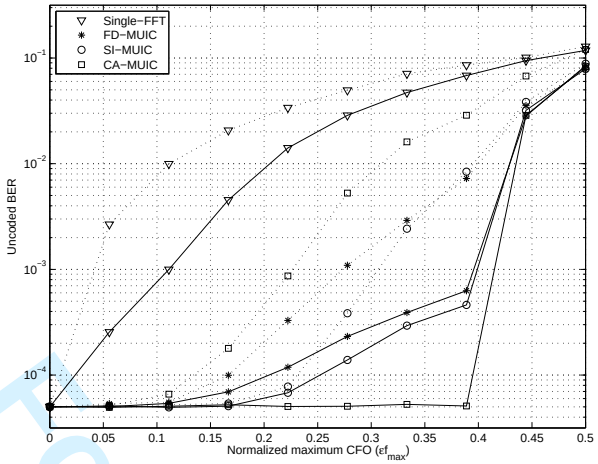

Fig. 6. Comparison of uncoded BER performances with different maximum CFO values. Solid line indicates block allocation, and dotted line represents interleaved allocation.

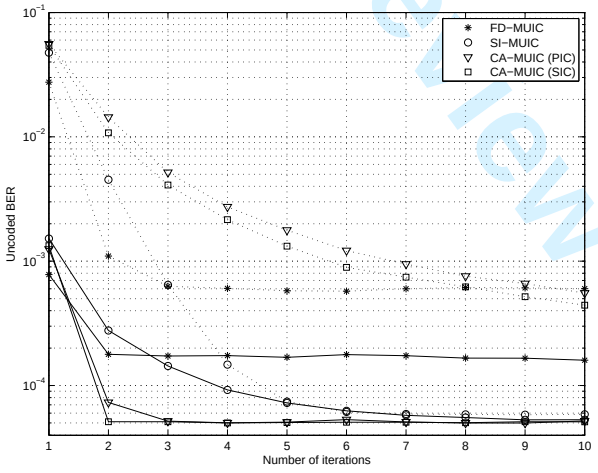

Fig. 7. Uncoded BER performances versus number of iterations. Solid line indicates block allocation, and dotted line represents interleaved allocation.

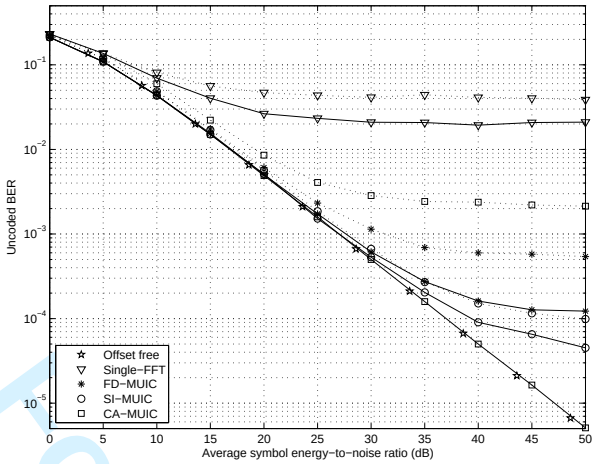

Fig. 8. Uncoded BER performances with different CNR values. Solid line indicates block allocation, and dotted line represents interleaved allocation.

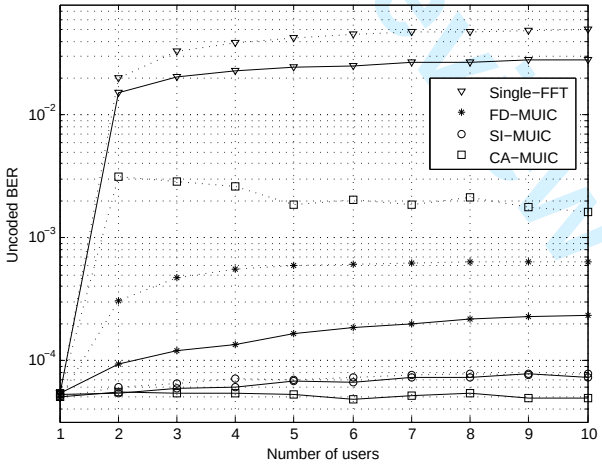

Fig. 9. Uncoded BER performance versus number of users. Solid line indicates block allocation, and dotted line represents interleaved allocation.

ANSWERS TO REVIEW'S QUESTIONS

Reviewer 1

Question 1: *The reviewer thinks that one major issue of these proposed schemes is the complexity. The multi-FFT receiver's complexity will be very high if the number of users and the number of subcarriers are relatively large. And the complexity of CA-MUIC will be much higher since it needs a extra IFFT for each user. Although Authors mention that the complexity is added only at BS, too much complexity is not applicable. Authors may need to provide the complexity comparison between different methods to show the equality.*

Answer: A complexity comparison between different methods has been introduced. We have added the following paragraphs in page 12; as well as Table I in page 19:

"The SI-MUIC scheme requires two FFT operations for each user in each iteration, one for demodulation and another for regenerating the corresponding time-domain signal. Therefore, the computation complexity of the SI-MUIC scheme is $\mathrm{O}(2UN_{loop}N\log_2 N)$, where $\mathrm{O}(.)$ and N_{loop} denote the order of complexity and number of iterations, respectively. Note that the SIC and PIC implementations are equivalent on complexity, as they require the same number of FFT operations per user per loop. The complexity of CA-MUIC scheme is larger than SI-MUIC, as decoding/coding, symbol demapping/mapping and channel insertion are involved. CA-MUIC's complexity is not accounted for in this paper, as it is considered only as an enhancement to SI-MUIC.

The FD-MUIC needs only one FFT operation at the beginning, but it requires U circular convolutions for each user in each iteration. The complexity of circular convolution can be reduced by considering only $P-1$ out of $N-1$ most dominant interfering subcarriers, at the cost of performance degradation [9]. The computation complexity of the FD-MUIC scheme in that case is $\mathrm{O}(UN_{loop}NP)$ [12], without considering the complexity of constructing the CFO correction matrices $\mathbf{C}_{(-\epsilon f_u)}$. Constructing CFO correction matrices requires computation of periodic sinc-function $\mathcal{C}(\phi)$, which can be costly and subjected to fixed-point precision problem. The CTYH scheme does not depend on the number of users and the number of iterations, but in principle it cost $\mathrm{O}(N^3)$ due to matrix inversion [12]. The complexity of the CTYH scheme can also be reduced by considering only $P-1$ most dominant interfering subcarriers, but the trade-off is performance degradation. Table I shows the number of arithmetic operations required for SI-MUIC, FD-MUIC and CTYH for different number of FFT size, where $U=10$ and $N_{loop}=5$. The complexity of the SI-MUIC is comparable to that of the FD-MUIC with $P=25$, while its performance exceeds that of the FD-MUIC with $P=N$."

Question 2: *If we do not consider the complexity, frequency compensation methods through linear*

multi-user detection was introduced in [2], which yield better performances than the scheme in [9]. Authors may need to compare the proposed schemes with the ones presented in [2]. It would be fairer to compare the two schemes with close complexity.

Answer: For completeness, we have included a performance comparison with the scheme in [2]. We introduce this scheme in page 3:

"A linear multiuser detection scheme is proposed in [2], hereby referred to as Cao-Tureli-Yao-Honan (CTYH), which attempts to restore the orthogonality among users by applying a linear transformation to the FFT output. The interference due to CFOs is suppressed at the price of additional complexity [12]."

And on page 7-8, a section for CTYH is presented, where the expression of the CINR corresponding to the scheme is given. We have also added the performance curve of the CTYH scheme in Fig. 2:

"The CTYH receiver is based on a single-FFT receiver, which aims at reconstructing the orthogonality among users in frequency-domain [2]. This goal is obtained by means of a linear transformation applied to:

$$\mathbf{Z} = \sum_{u=0}^{U-1} \mathbf{Z}_u = \mathbf{\Pi H X} + \mathbf{V} \tag{33}$$

where $\mathbf{Z}_u$ is defined in (5), $\mathbf{\Pi} = \sum_{u=0}^{U-1} \mathbf{C}_{(\epsilon f_u)} \mathbf{S}_u$ is the $N \times N$ interference matrix, $\mathbf{H} = \sum_{u=0}^{U-1} \mathbf{H}_u$ is CTF matrix and $\mathbf{X} = \sum_{u=0}^{U-1} \mathbf{X}_u$ is the transmitted symbol vector. The linear unbiased MMSE estimator [18] is chosen for performance comparison in section III-A.

The output CINR of the linear unbiased MMSE estimator at the k^{th} subcarrier is given by [18], [19]:

$$\text{CINR}_{MMSE,k}^{\text{CTYH}} = \frac{\sigma_X^2}{\left[(\mathbf{H}^H \mathbf{\Pi}^H \mathbf{\Pi H} + \frac{N_o}{\sigma_X^2}\mathbf{I})^{-1} N_o\right]_{kk}} - 1 \tag{34}$$

where all users transmit with equal power (i.e. $\sigma_{X_u}^2 = \sigma_X^2$ for all u) and $[.]_{kk}$ denotes the k^{th} diagonal element. It is worth noting that the CTYH receiver cannot achieve CFO-free performance, because it is based on a linear transformation technique."

Question 3: *Although the SIC may outperforms the PIC scheme, it will increase the complexity and process latency. Authors should mention this.*

Answer: The fact that SIC has longer processing latency are mentioned in page 10:

"Nevertheless, the SIC is penalized with a longer delay than PIC, since the last user can only be processed when all the others have been modulated."

On complexity, the SIC and PIC schemes require the same number of operation blocks, thus their complexity is equivalent. The difference between SIC and PIC is only the order of processing, i.e. SIC processes users one after another, while PIC processes all users simultaneously. To reflect this point in the paper, we have added the following sentence in page 12, section III-C:

"Note that the SIC and PIC implementations are equivalent on complexity, as they require the same number of FFT operations per user per loop."

Question 4: *In the middle of Page 11, Fig 5 is mistakenly noted as Fig??*

Answer: The missing number of the figure has been added.

Reviewer 2

Question 1: *It is better to give the references of conventional systems for the results given in Equation 5 and Equation 17*

Answer: References have been added for these two equations:

+ Equation 5: Reference to [2], [9]

+ Equation 17: Reference to [20]

Question 2: *Page 5 line after the equation 9 ,* $[.]^H$ *should be Hermitian transpose.*

Answer: The definition of $[.]^H$ has been re-defined as "Hermitian transpose".

Question 3: *Page 7 last line of the page 'the' is repeated twice.*

Answer: One "the" has been removed.

Question 4: *Page 9 line before the last line, it is not clear what is meant by "same OFDMA system's settings as in section II-B". Is it related to table 1 system parameters?*

Answer: No, the sentence "same OFDMA system's settings as in section II-B" is not related to Table 1 (system parameters) in section IV. It means "an OFDMA system with U=4, N=64 and fixed CFO as described in section II-B". The original text has been edited to make it more clear:

"Fig. 2 illustrates the convergence property of the SIC implementation of the SI-MUIC scheme, under the same OFDMA system's setting as in section II-B, where $U = 4$, $N = 64$ and the CFOs are fixed."

Question 5: *After the equation 27 Figure number is missing, which should be Fig.5.*

Answer: The missing number of the figure has been added.

Question 6: *Any suggestions if the number of carriers per user is not equal always. (Eg you have use here 200 carriers per each user).*

Answer: Both of the SI-MUIC and CA-MUIC schemes do not require each user to have an equal number of subcarriers. The SI-MUIC scheme should work well with any number of subcarriers, provided that the correct CFO estimates are available. For CA-MUIC scheme, the number of subcarrier dictates the coding length and diversity, therefore too few subcarriers allocated to a user can cause its performance to degrade. To reflex this explanation in the paper, we have added in page 15:

"Due to the limited space of the paper, we consider that each user is allocated the same number of subcarriers. However, the SI-MUIC scheme works well in any subcarrier allocation schemes, provided that the CFO estimates of users are available. The number of subcarriers dictates the coding length and the coding diversity for the CA-MUIC scheme, therefore too few subcarriers allocated to a user

can cause its performance to degrade. It is also worth noting that the interleaved subcarrier allocation scheme analyzed in this paper is considered as the worst case scenario for all the other allocation schemes."

Question 7: *What about CA-MUIC PIC implementation?*

Answer: The PIC implementation of CA-MUIC is added in page 11, and its performance is shown in Fig. 7:

"And the output of the CA-MUIC demodulator in case of the PIC implementation is given by:

$$\mathbf{Z}_{u,i}^{\mathrm{CA-MUIC,PIC}} = \mathbf{S}_u \left(\mathbf{Y}_u + \sum_{u_1=0; u_1 \neq u}^{U-1} \mathbf{C}_{(\epsilon f_{u_1-u}^{\mathrm{mFFT}})} \mathbf{I}_{u_1,i-1}^{\mathrm{CA-MUIC,PIC}} + \mathbf{C}_{(-\epsilon f_u)} \mathbf{V} \right) \tag{35}$$

$$\mathbf{I}_{u,i}^{\mathrm{CA-MUIC,PIC}} = \begin{cases} \mathbf{Y}_u & i = 0 \\ \mathbf{Y}_u - \mathbf{S}_u \hat{\mathbf{Y}}_{u,i}^{\mathrm{PIC}} & i > 0 \end{cases} \tag{36}$$

where $\hat{\mathbf{Y}}_{u,i}^{\mathrm{PIC}}$ is estimated from $\mathbf{Z}_{u,i}^{\mathrm{CA-MUIC,PIC}}$."

Question 8: *SIC shows its convergence properties: number of iterations for the given scenario is only 4-5. But as the number of users are increased this number of iterations can be large. Can the authors comment on this?*

Answer: We have removed the previous simulation results for 5 users and add new simulation results to cover a scenario with up to 10 users in Fig. 9. When the number of users are increased, only a insignificant performance degradation is observed with the same number of iterations. An explanation for this phenomenon has been added in page 14:

"Unlike in CDMA technique, the MUI in OFDMA does not increase linearly with the number of users, since the MUI caused by one subcarrier to another subcarrier decreases quickly as the distance between these two subcarriers increases [2]. Therefore, the performance of the SI-MUIC scheme is expected to change insignificantly when the number of users becomes greater than 10."

Question 9: *The convergence properties of CA-MUIC SIC are not presented.*

Answer: Fig. 7 has been added to show the convergence properties of both SIC and PIC versions of the CA-MUIC scheme. The following text is added on page 14:

"Fig. 7 shows the convergence properties of the CA-MUIC scheme, plotted along with the SIC implementation of FD-MUIC and SI-MUIC. In case of block allocation, the CA-MUIC converges faster than SI-MUIC, achieving the CFO-free performance in only two iterations. In interleaved allocation setting, it converges much slower than the SI-MUIC scheme. The main source of performance degradation in this case is error-propagation phenomenon: the applied convolutional code is not

strong enough to overcome large MUI from neighboring users, thus produce bit errors in detection, and those errors propagate from one iteration to the others. A stronger code is required to achieve better performance in interleaved subcarrier allocation scenario, or alternatively, the SI-MUIC can be applied in the first few iterations to clean up the received signal to a level for which the the CA-MUIC scheme can work effectively. Similar to SI-MUIC, the PIC implementation of the CA-MUIC scheme performs worse than its SIC version."

Question 10: *In page 7: a proper sentence is needed where authors mention: Defeng refers to the analysis provided in [9], while Huan refers to (15) - Since Huan presumably is one of the authors.*

Answer: The methods of CINR analysis for FD-MUIC have been re-named on page 7, and Fig. 1 is updated to reflect the name changed:

"Two methods of CINR analysis are compared to simulation results: Huang-Letaief (HL) refers to the analysis provided in [9], while Nguyen-Carvalho-Prasad (NCP) refers to (12). The methods are named after their authors, respectively."

Question 11: *Some change is spellings in words such as 'synchronis(z)ation' is needed.*

Answer: The spelling of the document has been changed to American-English style.